A Random Pore Model for Fluid-Solid Reactions: I. Isothermal, Kinetic Control

S. K. BHATIA

and

D. D. PERLMUTTER

Department of Chemical Engineering
University of Pennsylvania
Philadelphia, Pennsylvania 19104

For fluid-solid reactions, a random pore model is developed which allows for arbitrary pore size distributions in the reacting solid. The model can represent the behavior of a system that shows a maximum in reaction rate as well as one that does not, and it identifies an optimal pore structure for either of such systems. It is demonstrated that the new model subsumes several earlier treatments as special cases. By comparison with the grain model, a relationship is derived between the effective grain shape factor and a pore structure parameter defined here. When the variance of the pore size distribution is effectively zero, the new results approach those predicted by the Petersen 1957 model over a large range of conversions. The char gasification data of Hashimoto et al. (1979) are shown to produce correlations consistent with the expectations of the new model.

SCOPE

A random pore model is developed in terms of a pore size distribution in the reacting solid. A maximum in reaction rate is found to exist for some values of the system parameters, but not for others. This result is consistent with experimental reports and shows the new model to be more flexible than either grain models or order of reaction models from which only reaction rate decreases can be expected with increase in conversion.

The new model utilizes a pore structure parameter to characterize solid reactivity, and the analysis relates this parameter to m, the grain shape factor or order of reaction used in prior models. This approach offers a likely explanation for the commonly reported variations in m, even among tests run on the same substances.

CONCLUSIONS AND SIGNIFICANCE

A comparison of the proposed random pore model with a prior grain model shows that m, the effective grain shape factor or order of reaction, is intimately related to the pore structure of the solid. The volume reaction model ($m = 1$) arises as a limiting case; however, the new model is not consistent with the assumption of flat plate grains ($m = 0$) for any pore structure. The results indicate that for certain pore characteristics, a rate maximum may be observed with increasing conversion. The initial increase in rate is attributed to the growth of reaction surfaces from the initial pores. This effect is overshadowed in later stages by the intersections of the growing surfaces which act to decrease reaction rate.

It is shown that, in general, the three parameters of pore volume, surface area, and length are needed to adequately characterize the structure when an arbitrary pore size distribution exists; however, two parameters may be sufficient in special cases. Comparison with the Petersen model (1957) shows that the two models can be in agreement, but only for the special case of uniform pore size. Even then, however, some deviation between the prior model and the new one is found at high conversions (above about 75%), probably because of the neglect of new intersections of reaction surfaces in the Petersen approach. By using the characteristic parameters of a random pore size distribution, the proposed model avoids the need to assume an idealized structure having uniformly sized cylindrical pores, nor does it neglect the intersection of reaction surfaces as they grow (Petersen, 1957; Ramachandran and Smith, 1977). Furthermore, by interpreting grain models in terms of a pore structure, these contrasting approaches are unified.

One of the important features of the proposed model is that it predicts the reaction surface area at any given conversion as a function of an initial pore structure parameter. This makes possible explanation of the strong influence of the initial pore structure that has been experimentally observed in a number of investigations (Dutta et al., 1977; Dutta and Wen, 1977; Hashimoto et al., 1979).

In modeling fluid-solid reactions, it is common to consider the reaction as occurring on internal surfaces of the solid. The models can be classified into two categories: those that consider the reaction on the surfaces of nonporous grains, and those that emphasize instead the reaction initiated on pore surfaces within the solid. Representative of models in the former category are the treatments of Calvelo and Smith (1971) and Szekely and Evans (1970), who consider the shrinking core behaviors of uniformly sized nonporous grains of the reactant solid. For the reaction

$$aA(g) + bB(s) \rightarrow pP(g) + qQ(s) \qquad (1)$$

0001-1541-80-3242-0378-$00.95.

in the regime of chemical reaction control, the result for such models expresses the reaction rate as

$$\frac{dX}{dt} = \frac{k_s C^n S_o}{(1 - \epsilon_o)} (1 - X)^m \tag{2}$$

where m is identified as a shape factor that depends on the geometry of the grains: for spheres $m = 2/3$, for cylinders $m = ½$ and for flat plates $m = 0$. Other equivalent representations which treat m as an order of reaction have also been suggested. For $m = 1$, Equation (2) corresponds to the so-called volume or pseudo-homogeneous reaction model of Lacey et al. (1965) and Ishida and Wen (1971). Equation (2) incorporates the structural parameters of the solid in terms of porosity and surface area; however, it predicts a monotonically decreasing reaction rate because the reacting surface of each grain is receding. Some systems, notably gasification reactions (Dutta et al., 1977; Dutta and Wen, 1977), exhibit a maximum in the reaction rate. This is generally attributed to an increase in the reacting surface area during the early stages of the reaction, a view supported by the measurements of Kawahata and Walker (1962) and Hashimoto et al. (1979) for activated carbons. The grain model does not account for such changes in structure occurring during the reaction of the solid. A variation of the spherical grain model has also been suggested by Park and Levenspiel (1976); their crackling core representation does allow for sigmoidal conversion-time curves through the use of an added fitting parameter.

Models that analyze the pore structure commonly include the assumptions that all pores are of the same size and that no new intersections occur as the reaction surfaces within the solid particle grow. One such model is that of Petersen (1957), who analyzed the complete gasification of a solid assumed to be comprised of cylindrical pores of uniform radius r_p. Because no solid product is formed in complete gasification of a pure reactant, the reaction surface of the solid is always the same as the internal surface of the pores, and the porosity is the volume enclosed by the reaction surface. Petersen's results are

$$S = 2\pi r_p L(1 - r_p \sqrt{\pi L/3}) \tag{3}$$

$$\epsilon = \pi r_p^2 L \left(1 - \frac{2r_p}{3}\sqrt{\pi L/3}\right) \tag{4}$$

and with local rate of reaction proportional to surface area, the rate of pore growth is

$$\frac{dr_p}{dt} = k_s C^n \tag{5}$$

Using Petersen's formulations and neglecting reaction on the external surface, Szekely et al. (1976) have derived the conversion-time relationship for the kinetic regime to be

$$X = \frac{\epsilon_o}{(1 - \epsilon_o)} \left[\left(1 + \frac{k_s C^n t}{r_{po}}\right)^2 \frac{\left(G - 1 - \dfrac{k_s C^n t}{r_{po}}\right)}{G - 1} - 1 \right] \tag{6}$$

where G is the solution to the cubic equation

$$\frac{4}{27}\epsilon_o G^3 - G + 1 = 0 \tag{7}$$

An extension to the case of formation of a solid product was provided by Calvelo and Cunningham (1970). A more recent structural model of Ramachandran and Smith (1977) also considers the solid to be comprised of cylindrical pores of uniform size and neglects the intersections as the reaction surface grows.

Hashimoto and Silveston (1973) adopted a population balance technique and accounted for the distribution in pore sizes as well as the collapse of pore walls into each other as reaction proceeds. The model includes two parameters, which pertain to the intersection of reaction surfaces as they grow, that are to be estimated from the conversion behavior of the solid. As a consequence, the model does not readily lend itself to the a priori prediction of conversion-time data from kinetic information and measurable structural properties of the solid alone.

In comparing the various models for pore reactions, it is valuable to consider also direct physical measurements of pore structure. By combining mercury porosimetry with adsorption methods, Walker and Raats (1956), in studies with graphitized carbon rods, obtained mean pore radius, surface area and pore volume as independent parameters. Using similar methods, Kawahata and Walker (1962) determined initial pore volume, surface area and length as three independent characteristics of a sample of unactivated anthracite coal. Alternatively, any two of these three parameters may be replaced by a mean pore radius and a variance of radii. This alternative is especially attractive in a case where the pores are uniform and the variance may be taken as zero. This is, in effect, the model used by Petersen and is consistent with his Equations (3) and (4), which describe the structure in terms of only the two parameters, pore radius and total length.

In the development that follows, a general model is presented that accounts for the random overlap of reacting surfaces as they grow by extending a theory originally developed by Avrami (1940) for the analysis of the geometry of crystal aggregates. No assumption is needed as to the actual shapes of the pores.

MODEL DEVELOPMENT

Consider the isothermal chemical reaction of particles of the solid B with a fluid A according to the stoichiometry of Equation (1). The reaction is initiated on the surfaces of pores in the solid B. As further reaction occurs, a layer of product Q is formed around each pore which separates the growing reaction surface of the solid B from the fluid reactant A within the pores. Reactant A diffuses through the product layer to the reaction surface where chemical change occurs. If all diffusional resistances are assumed negligible, no distinction need be made between macro and micropores (the kinetic regime). It is assumed that the reactant B has no significant closed pore volume.

As reaction progresses, each pore of the particle has associated with it a growing reaction surface which initially corresponds to the inner surface of the pore. As the various reaction surfaces in the particle grow, it is inevitable that neighboring surfaces will intersect one another as the solid B separating them is consumed and replaced by the product Q.

Consider the actual reaction surface of the solid B at any time to be the result of the random overlapping of a set of cylindrical surfaces of size distribution $f(r)$, where $f(r)dr$ is the total length of the cylindrical surfaces per unit volume of space having radii between r and $r + dr$. Define

$$L_E = \int_0^\infty f(r)dr \tag{8}$$

$$S_E = 2\pi \int_0^\infty rf(r)dr \tag{9}$$

and

$$V_E = \pi \int_0^\infty r^2 f(r)dr \tag{10}$$

as the total length, total surface area and total enclosed volume of the nonoverlapped cylindrical system. A balance over the size distribution of the growing cylinders yields

$$\frac{\partial f}{\partial t} + \frac{\partial}{\partial r}\left[f\frac{dr}{dt}\right] = 0 \tag{11}$$

where it is assumed that no cylinders are created or destroyed.

The growth of the total reaction surface may be followed in terms of the radial growth of a given set of overlapping cylinders, as shown in Figure 1. If the rate of reaction on the actual surface is proportional to the total surface area

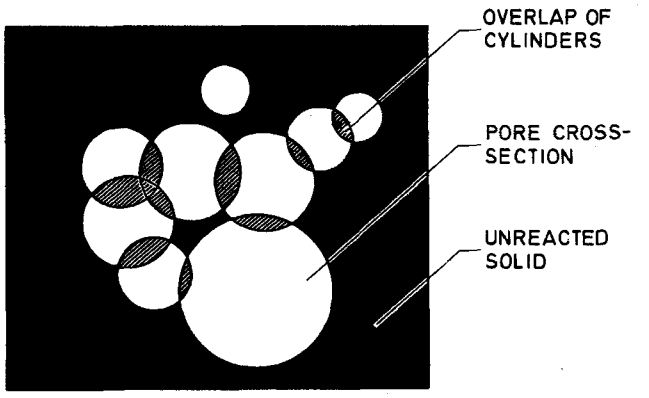

Figure 1. Overlapping of cylindrical surfaces. The hatched area shows the overlapped portion. The blackened area represents unreacted solid B. The reaction surface is the interface between the nonoverlapped portion of the cylindrical surface and the unreacted solid. The product layer that is deposited as the reaction surface moves is not shown in this figure. (After Avrami)

$$\frac{dr}{dt} = k_s C^n \tag{12}$$

because each element of the actual surface must belong to the nonoverlapped portion of some cylinder. Combining Equations (11) and (12), we get

$$\frac{\partial f}{\partial t} = -k_s C^n \frac{\partial f}{\partial r} \tag{13}$$

Integrating Equation (13) with respect to r, and using Equation (8) together with the conditions $f(0) = f(\infty) = 0$, we get

$$\frac{dL_E}{dt} = 0 \tag{14}$$

Multiplying Equation (13) by $2\pi r$, integrating with respect to r and inserting definitions (8) and (9), we get

$$\frac{dS_E}{dt} = 2\pi k_s C^n L_E \tag{15}$$

Similarly, if we multiply Equation (13) by πr^2, integrate with respect to r and substitute Equation (10), an equation for the total volume is obtained in the form

$$\frac{dV_E}{dt} = k_s C^n S_E \tag{16}$$

Equations (14), (15) and (16) can be solved to yield

$$S_E = \sqrt{S_{Eo}^2 + 4\pi L_{Eo}(V_E - V_{Eo})} \tag{17}$$

and

$$V_E = V_{Eo} + S_{Eo}(k_s C^n t) + \pi L_{Eo}(k_s C^n t)^2 \tag{18}$$

which describe the evolution of the nonoverlapped surface and volume as conversion proceeds. It remains to relate these quantities to the corresponding properties of the actual (or overlapped) surface. To this end, consider the growth in the volume enclosed by the nonoverlapped surface. Avrami (1940) has shown in a slightly different context that on the average the increment in the volume enclosed by the actual (or overlapped) system is only a fraction of the growth in the nonoverlapped cylindrical system. Moreover, this fraction is $(1 - V)$, the fractional volume of space occupied by the unreacted solid B; that is

$$dV = (1 - V)dV_E \tag{19}$$

This result of Avrami's has formed the basis of several models for solid phase reactions (Young, 1966; Tompkins, 1976) where it is assumed that reaction is initiated at discrete nucleus forming sites, and that nuclei overlap as they grow. Bhatia and Perlmutter (1979) have pointed out that this relationship, which represents a statistical average, may not be sufficiently accurate in the initial stages of a solid phase reaction when the number of nuclei is small; however, in the present context, where the reacting surface starts out with an extensive system of reaction surfaces, it should suffice to follow the mean value of dV through Equation (19).

With the observation that $V \to 0$ as $V_E \to 0$, Equation (19) can be integrated to

$$V = 1 - \exp(-V_E) \tag{20}$$

To obtain a relationship between the surface areas of the overlapped and nonoverlapped systems, consider the increase in volume of the overlapped system by an amount dV in time dt. Since the rate of reaction is assumed proportional to surface area

$$dV_E = S_E(k_s C^n)dt \tag{21}$$

and

$$dV = S(k_s C^n)dt \tag{22}$$

Combining Equations (19), (21) and (22), we get

$$S = S_E(1 - V) \tag{23}$$

As the overlapped system increases in volume by an amount dV, the change in the total length of the system due to additional intersections may be written as

$$dL = -\frac{L}{(1 - V)}dV \tag{24}$$

Since no overlapping is possible at $V = 0$

$$\lim_{V \to 0} L = L_E \tag{25}$$

Integrating Equation (24) with boundary condition (25), we obtain

$$L = L_E(1 - V) \tag{26}$$

Combining Equations (20), (23) and (26) with Equations (17) and (18), we get

$$\frac{S}{S_o} = \left(\frac{1 - V}{1 - V_o}\right)\sqrt{1 - \frac{4\pi L_o(1 - V_o)}{S_o^2}\ln\left(\frac{1 - V}{1 - V_o}\right)} \tag{27}$$

$$V = 1 - (1 - V_o)\exp\left[-\frac{k_s C^n t}{(1 - V_o)}(S_o + \pi L_o k_s C^n t)\right] \tag{28}$$

For a spherical particle in the regime of reaction control

$$1 - X = \left(\frac{1 - V}{1 - V_o}\right)\left(1 - \frac{k_s C^n t}{R_o}\right)^3 \tag{29}$$

In dimensionless form, Equations (27) and (28), upon combining with Equation (29) and the initial condition

$$V_0 = \epsilon_o \tag{30}$$

become

$$\frac{S}{S_o} = \frac{1 - X}{\left(1 - \frac{\tau}{\sigma}\right)^3}\sqrt{1 - \psi \ln\left[\frac{1 - X}{\left(1 - \frac{\tau}{\sigma}\right)^3}\right]} \tag{31}$$

and

$$X = 1 - \left(1 - \frac{\tau}{\sigma}\right)^3 \exp\left[-\tau\left(1 + \frac{\psi\tau}{4}\right)\right] \tag{32}$$

RESULTS AND DISCUSSION

Conversion-Time Behavior

Equation (32) provides conversions at each dimensionless time in terms of the initial pore structure parameter ψ and the particle size parameter σ. Typical order of magnitude values for common porous solids are

$$S_o = 10^4 \text{ cm}^2/\text{cm}^3$$

$$L_o = 10^7 \text{ cm/cm}^3$$

$$\epsilon_o = 0.3$$

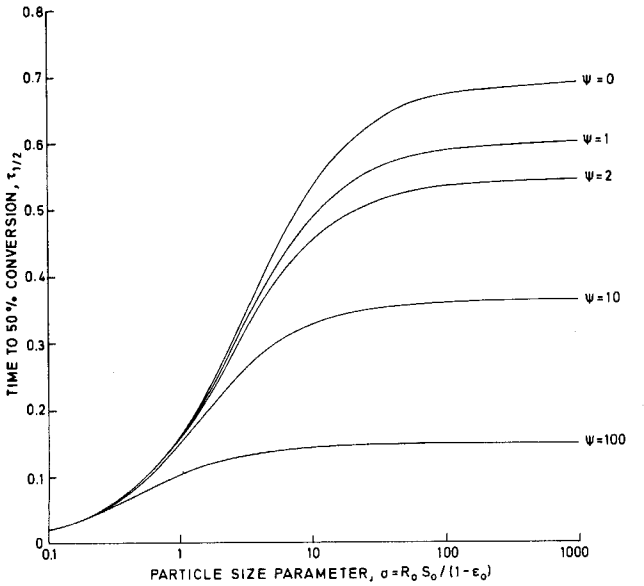

Figure 2. The effect of particle size on time required for 50% conversion for various values of the pore structure parameter.

$$R_o \geq 10^{-2}\,\text{cm}$$

From these numerical choices, ψ is of the order of 1, and $\sigma > 100$. To characterize the effect of particle size, it is convenient to use Equation (32) to compute the time required for 50% conversion at various levels of ψ. Such results are presented in Figure 2, from which it is evident that no further significant change occurs for $\sigma \geq 100$. In effect, the particle external surface is negligible in comparison with the internal pore surface. The opposite effect is also observable in Figure 2. For small enough particles ($\sigma < 0.25$), the reaction time is independent of internal structure for $\psi \leq 100$. Between the limits there is a transition region in which both internal and external surfaces are of comparable influence. In the range of parameters where the external surface is negligible, the choice of $\sigma = \infty$ is a convenience, and the conversion-time curve may be computed for each choice of the pore structure parameter. Such results are presented as Figure 3, from which one can note that the rate (slope) usually decreases with conversion as wall collapse progressively acts to reduce the total reaction surface area. For the higher levels of ψ, this process is delayed until relatively higher conversions, and the overall effect is more affected by the growth of reaction surfaces associated with the pores.

Reaction Surface

Equation (31) relates the reaction surface area to the conversion in terms of the pore structure and particle size parameters. The results shown for $\sigma \to \infty$ in Figure 4 indicate that a maximum surface occurs when the value of the parameter ψ is large, but not for small values. The maximum arises from the two opposing effects: the growth of reaction surfaces associated with the pores and the loss of these surfaces as they progressively collapse by intersection. The latter effect overshadows the first at all levels of conversion when the pore structure parameter is small enough.

By differentiating Equation (31), the conversion corresponding to the maximum surface for $\sigma \to \infty$ is obtained as

$$X_M = 1 - \exp[(2 - \psi)/2\psi] \qquad (33)$$

This maximum exists over the range $2 \leq \psi < \infty$ and gives $0 \leq X_M < 0.393$. For comparison, the data of Walker and Raats (1956) indicate a maximum in surface area at about 34.5% conversion. The role of diffusion in their experiments is not clearly indentified, but it should be noted that this treatment is valid only in the kinetically controlled regime and in the absence of new pore

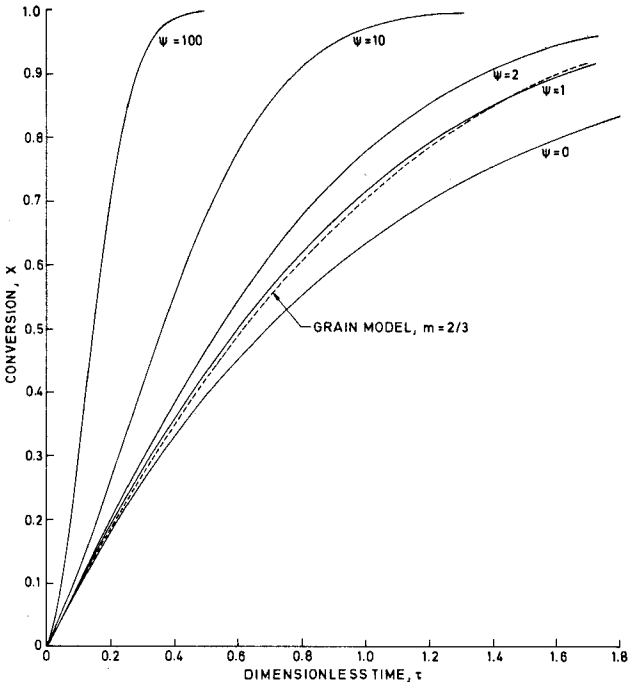

Figure 3. The effect of reaction time on overall conversion for different pore structures with negligible external surface; dashed line is result of grain model with $m = 2/3$.

generation. The data of Kawahata and Walker (1962) show a maximum in surface area at about 40 to 50% conversion, but their reactant solid had a large closed pore volume, over 60% of the open pore volume. The experiments of Dutta et al. (1977) and of Dutta and Wen (1977) on the reactivity of various chars

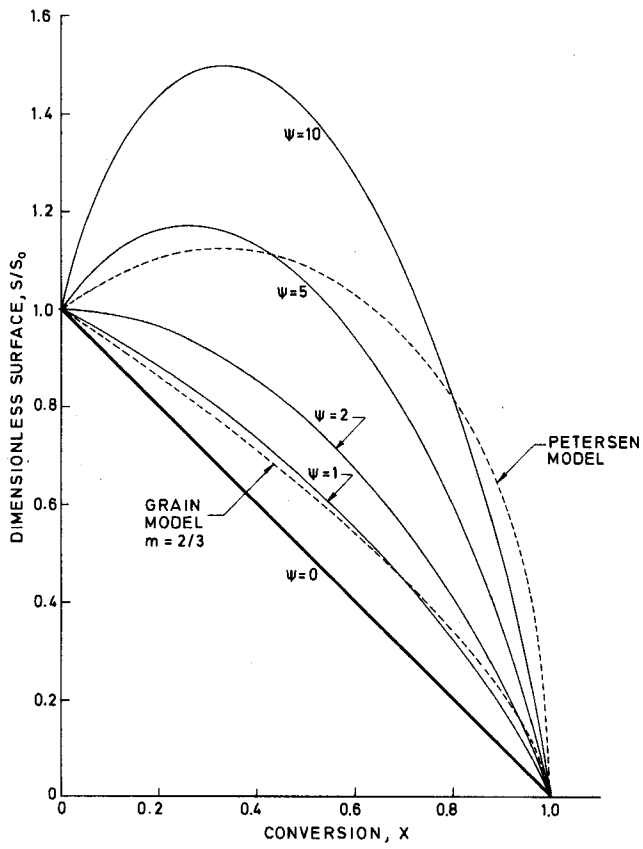

Figure 4. Development of the reaction surface with conversion according to the random pore model, compared with grain model for $m = 2/3$ and Petersen model for $\epsilon_0 = 0.26$, $L_0 = 3.14 \times 10^6$ cm/cm^3, $S_0 = 2{,}425$ cm^2/cm^3.

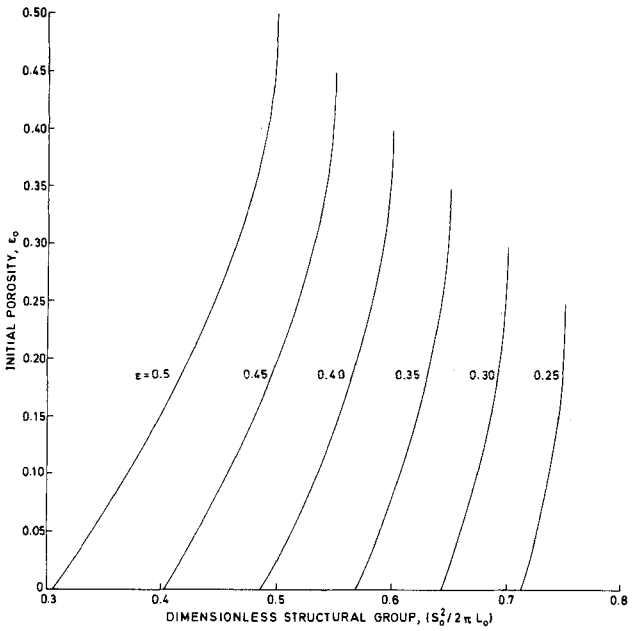

Figure 5. Variation of optimal initial porosity with structural group ($S_o^2/2\pi L_o$) for different values of desired porosity ϵ.

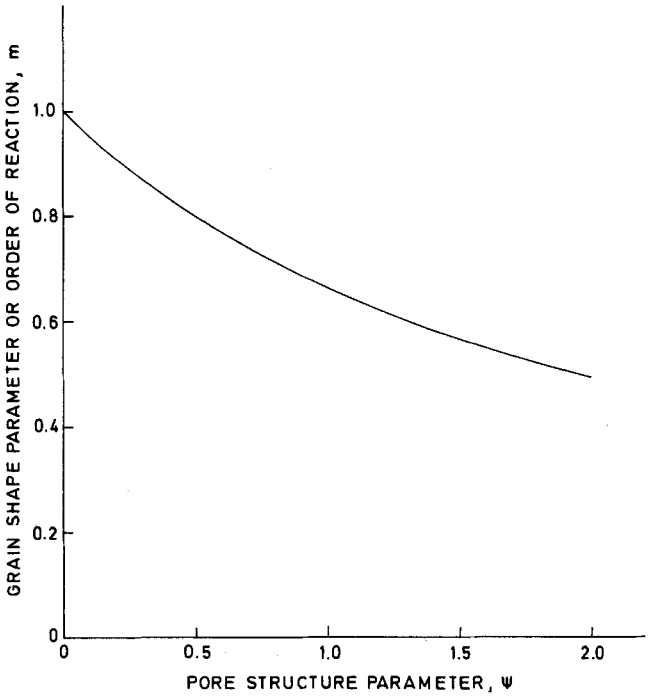

Figure 6. Best fit values of m for various choices of the pore structure parameter ψ.

also show a maximum in the reaction rate at conversions below $X = 0.4$.

The comparable results of the Petersen model may be derived from Equations (3) to (7) to give

$$X_M = \frac{1 - 2\epsilon_o}{2(1 - \epsilon_o)} \tag{34}$$

From this equation, a rate maximum requires $0 \leq \epsilon_o \leq 0.5$ and can vary between $0 \leq X_M \leq 0.5$. The model developed here uses the structural parameter to include in the criterion L_o and S_o in addition to the porosity ϵ_o.

Optimal Structure

There is evidence in the work of Yamadaya et al. (1970) that when solids of a fixed grain size are compacted under various pressures, the porosity varies, although other structural parameters do not change. In cases where such a pattern is available, the foregoing relationships can also be used to determine an initial pore structure that will produce a maximum surface for a specified final porosity. The required optimal initial porosity can be obtained by maximizing the surface area in Equation (27) with respect to V_o, at constant S_o and L_o. If we assume that the application is to a reaction having no solid product, $\epsilon = V$ and the differentiation gives

$$\frac{S_o^2}{2\pi L_o(1 - \epsilon_o)} = 1 + \ln\left(\frac{1 - \epsilon}{1 - \epsilon_o}\right) \tag{35}$$

Numerical values obtained from this equation are shown in Figure 5, from which it is evident that a particular specification of ϵ can only be reached from a restricted range of initial settings:

$$[1 + \ln(1 - \epsilon)] \leq \frac{S_o^2}{2\pi L_o} \leq [1 - \epsilon] \tag{36}$$

If, for example, a final $\epsilon = 0.3$ is sought for a solid where $(S_o^2/2\pi L_o) = 0.67$, the initial ϵ_o should be 0.1 to maximize the final surface area. If the value of $(S_o^2/2\pi L_o) \leq 0.64$, inequality (36) is violated, and there is no ϵ_o that will produce a maximum area at $\epsilon = 0.3$.

Comparison With Other Models

The model developed here has the facility of describing systems with or without maxima in reaction rate. In this regard, it is more flexible than those models based on an order of reaction or a grain model [Equation (2)]. The Petersen model [Equations (3) to (7)] can describe either kind of behavior, too; however, it makes no provision for further pore wall intersections and neglects the distribution of pore sizes.

To draw a comparison between the results developed here and those of the earlier models, it is convenient to differentiate Equation (32) as $\sigma \to \infty$ to give

$$\frac{dX}{d\tau} = (1 - X)\sqrt{1 - \psi \ln(1 - X)} \tag{37}$$

This reduces exactly to the volume reaction model if $\psi = 0$. For nonzero values of ψ, the volume reaction model will still be a good approximation for all X such that

$$\psi \ln\left(\frac{1}{1 - X}\right) << 1 \tag{38}$$

In terms of the grain model, the rate Equation (2) may be written in dimensionless form as

$$\frac{dX}{d\tau} = (1 - X)^m \tag{39}$$

For spherical grains, $m = 2/3$, giving the results superimposed as the dashed line in Figure 4. If Equation (39) is integrated to

$$X = 1 - \left(1 - \frac{\tau}{3}\right)^3 \tag{40}$$

the comparison can also be made in terms of the dashed line in Figure 3. In either figure, it is clear that the grain model predictions match the $\psi = 1$ results within the limits of the usual experimental error. This match at $m = 1$ combined with the above-mentioned correspondence as $\psi \to 0$ suggests that the concept of reaction order with respect to the fraction of unconverted solid is intimately associated with its pore structure. Such a view would explain some of the discrepancies reported by even the most careful workers. In studies of the oxidation of zinc sulfide, for example, Takamura et al. (1974) reported good fit of the volume reaction model ($m = 1$) for their porous particles, while Mendoza et al. (1970) demonstrated the validity of the spherical grain model ($m = 2/3$). In investigations of the reduction of nickel oxide by hydrogen, Szekely and Evans (1971) were able to show data fit with $m = 2/3$; in other experiments Szekely et al. (1973) also report $m = ½$ but argue that the assumption of cylindrical grains is probably poor. Barner and

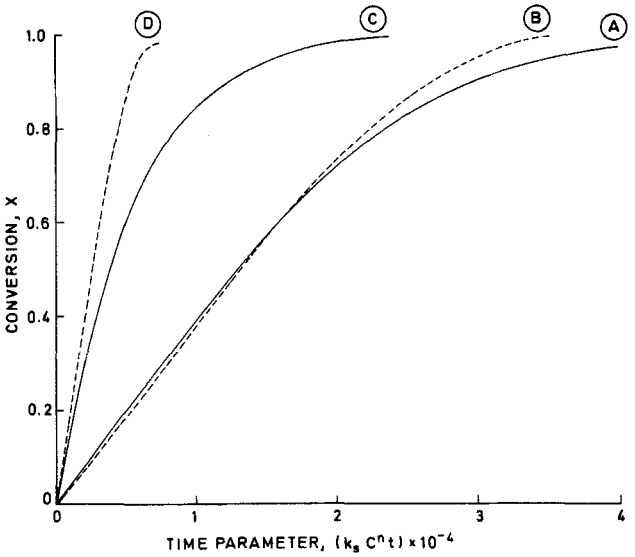

Figure 7. Comparison between random pore and Petersen models; curves A and C are for random pore model, curves B and D are for Petersen model; for all calculations, $\epsilon_o = 0.3$; parameters used for curves A and B are S_o = 2 500 cm²/cm³, $L_o = 3.14 \times 10^6$ cm/cm³; for curve C, S_o = 12 500 cm²/cm³, $L_o = 3.14 \times 10^6$ cm/cm³; for curve D, S_o = 12 500 cm²/cm³ and L_o is internally calculated via Equations (3) and (4).

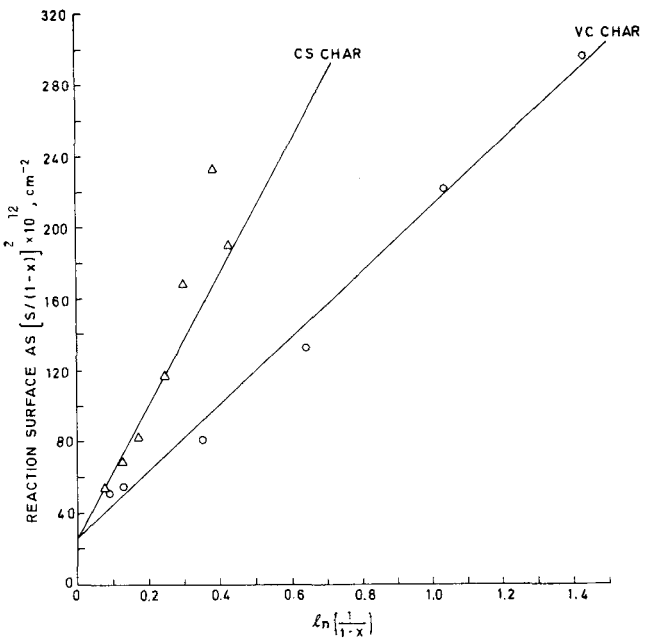

Figure 8. Correlation of the data of Hashimoto et al. (1979) with random pore model.

Mantell (1968) assumed cubical grains in their study of manganese dioxide reduction, and obtained $m = 2/3$ experimentally.

Comparing the competing models, we can expect that a best value of m can be found to fit the interpretation of Equation (37) to the functional form provided by Equation (39) with a given choice of ψ. If this best fit is defined to minimize the squared deviations integrated over the full conversion range

$$I = \int_0^1 [(1 - X)^1 \sqrt{1 - \psi \ln(1 - X)} - (1 - X)^m]^2 dX$$

the results can be presented as in Figure 6. For $0 \leq \psi \leq 2$, the best fit gives $0.49 \leq m \leq 1$. For $\psi = 1$, the best m is very close to two-thirds, as anticipated from Figures 3 and 4. It appears, however, that the choice of $m = 0$ (that is, flat plate grains) would be a grossly inadequate fit for any ψ if applied over a large conversion range. Further, it should be emphasized that the order of reaction model cannot under any circumstance represent a rate maximum such as must develop when $\psi > 2$.

To compare the results of this study with those of Petersen (1957), consider a pore structure with parameters that satisfy Equations (3) and (4):

$$S_o = 2{,}425 \text{ cm}^2/\text{cm}^3$$

$$L_o = 3.14 \times 10^6 \text{ cm/cm}^3$$

$$\epsilon_o = 0.26$$

The relative reaction surface may be calculated by differentiating Equation (6) and this Petersen result superimposed on the family of constant ψ curves in Figure 4. From its definition, the chosen parameters give $\psi = 5$. The agreement is, in general, only fair, the discrepancy between the two models becoming larger with high conversion where the intersections between reacting surfaces are expected to play a greater role.

Another form of comparison is presented in Figure 7 as superimposed conversion-time curves for three different sets of parameters. Curves A and B are in good agreement up to about 75% conversion and diverge thereafter because the Petersen model does not attempt to account for the collapse of reaction surface. Both curves are based on parameter choices that satisfy Petersen's Equations (3) and (4) and consequently assume implicitly that the pore distribution has zero variance.

The curve C is based on system constants no longer consistent with the requirements of Petersen's model:

$$S_o = 12{,}500 \text{ cm}^2/\text{cm}^3$$

$$L_o = 3.14 \times 10^6 \text{ cm/cm}^3$$

$$\epsilon_o = 0.3$$

The corresponding Petersen choices are not, in this case, uniquely defined. If $\epsilon_o = 0.3$ and $L_o = 3.14 \times 10^6$ are chosen, the results are the same as the prior curve B. If, on the other hand, $\epsilon_o = 0.3$ and $S_o = 12{,}500$ cm²/cm³ are fixed, curve D is obtained. Neither curve B nor D are in agreement with the result C because the restrictions of the Petersen model do not account for the pore size distribution.

Correlation of Experimental Data

The three parameters ϵ_o, S_o and L_o are the core features of the proposed model. Usually, the initial porosity ϵ_o is directly determinable, and S_o and L_o must be estimated from other measurements. One such technique (Szekely et al., 1976) uses electron microscopy to view a sample cross section of the solid to count pores in various size ranges, but this is a very tedious method. More convenient direct determination of an initial pore volume distribution $v_o(r)$ is possible by mercury penetration porosimetry if the sizes are known corresponding to penetration at each applied pressure. The three parameters of interest are then obtainable from

$$\epsilon_o = \int_o^\infty v_0(r) dr \tag{41}$$

$$S_o = 2 \int_0^\infty \frac{v_o(r)}{r} dr \tag{42}$$

$$L_o = \frac{1}{\pi} \int_o^\infty \frac{v_o(r)}{r^2} dr \tag{43}$$

An estimate of the surface area S_o is also obtainable by BET gas adsorption. An illustration of the use of these methods is offered in the work of Kawahata and Walker (1962), who combined porosimetry with adsorption methods to estimate ϵ_o, S_o and L_o for their anthracite.

When porosimetry data are not conveniently available, reaction studies under kinetic control can also be utilized to estimate the desired quantities. Such studies have been conducted by

Szekely et al. (1973) in connection with the determination of the parameters of the grain model. In the present context, measurements of relative reaction rate (effectively, measurements of reaction surface area when no solid product is formed) may be utilized to determine ψ by applying Equation (31).

As an example of the use of the above technique, consider the data of Hashimoto et al. (1979) on the reaction developed BET surface areas produced by steam activation of chars from three sources: coconut shell (CS), Victoria coal from Australia (VC) and Miike coal from Japan (MC). Of these, the CS and VC materials have very small mineral matter content (2 to 3%) and negligible closed pore volume, providing data most suitable for correlation by the model under consideration. For these chars, the authors have provided information on the weight fraction of mineral matter, bulk density of the chars and BET surface area per unit mass of starting material at varying levels of fractional weight change X_c. To adapt their data to the present purpose, it is necessary to calculate conversions and surface areas by the equations

$$X = 1 - \frac{\rho_b}{\rho_{bo}}\left(\frac{1-\omega}{1-\omega_o}\right) \tag{44}$$

and

$$S = \frac{\rho_b S_B}{1 - X_c} \tag{45}$$

Then, as $\sigma \to \infty$, Equation (31) predicts a linear semilog relationship between the group $[S/(1-X)]^2$ and $(1-X)$. This expectation is supported by the data within the limits of experimental error, as shown in Figure 8. Estimates of initial BET surface areas obtained from the intercept of Figure 8 give 520 m^2/cm^3 for both VC and CS char. The two slopes give $\psi = 6.9$ and $\psi = 13.7$ for the VC and CS chars, respectively. Since both values are greater than $\psi = 2$, maxima in the surface areas may be expected. This was, in fact, reported in the reference work for the CS char but did not show up for the VC char, obscured by the particle attrition that occurred in the fluidized bed used.

Thiele moduli based on the initial surface areas are small enough to assure effectiveness factors over 0.98 in all cases, justifying the assumption of kinetic control.

ACKNOWLEDGMENT

This research was support by the U.S. Department of Energy, Office of Basic Energy Science under Contract No. EY-76-S-02-2747. The authors are grateful to Professor K. Hashimoto of Kyoto University, who supplied the data on the chars referred to in the last section.

NOTATION

a, b = stoichiometric coefficients
C = concentration of gaseous reactant A
$f(r)$ = size distribution of nonoverlapped system at any time
G = quantity defined by Equation (7)
k_s = rate constant for surface reaction
L = length of overlapped system
L_E = total length of nonoverlapped system
L_{Eo} = L_E at $t = 0$
m = grain shape factor, or reaction order with respect to solid B
n = reaction order with respect to gas A
p,q = stoichimetric coefficients
r = radius of cylindrical surface
r_p = pore radius in Petersen's model
r_{po} = r_p at $t = 0$
R_o = initial particle radius
S_B = BET surface area per unit mass of starting material
S = reaction surface area per unit volume
S_o = S at $t = 0$
S_E = surface area of cylindrical system, per unit volume
S_{Eo} = S_E at $t = 0$
t = time
V = volume enclosed by reaction surface, per unit volume of space
V_o = V at $t = 0$
V_E = volume enclosed by cylindrical system, per unit volume of space
V_{Eo} = V_E at $t = 0$
X = conversion
X_M = conversion at time of maximum surface

Greek Letters

ϵ = porosity
ϵ_o = initial value of ϵ
ψ = $4\pi L_o(1-\epsilon_o)/S_o^2$, structural parameter
ρ_b = bulk density of char
σ = $R_o S_o/(1-\epsilon_o)$, particle size parameter
τ = $k_s C^n S_o t/(1-\epsilon_o)$, dimensionless time
ω = weight fraction of mineral matter in char

LITERATURE CITED

Avrami, M., "Kinetics of Phase Change. II. Transformation—Time Relations for Random Distribution of Nuclei," *J. Chem. Phys.*, **8**, 212 (1940).

Barner, H. E., and C. L. Mantell, "Kinetics of Hydrogen Reduction of Manganese Dioxide," *Ind. Eng. Chem. Process Design Develop.*, **7**, 285 (1968).

Bhatia, S. K., and D. D. Perlmutter, "A Population Balance Approach to the Modeling of Solid Phase Reactions," *AIChE J.*, **25**, 298 (1979).

Calvelo, A., and R. E. Cunningham, "Kinetics of Gas-Solid Reactions," *J. Catalysis*, **17**, 1 (1970).

Calvelo, A., and J. M. Smith, "Intrapellet Transport in Gas-Solid Non-Catalytic Reactions," *Proceedings of Chemeca 70*, paper 3.1, Butterworths, Australia (1971).

Dutta, S., C. Y. Wen and R. J. Belt, "Reactivity of Coal and Char. I. In Carbon Dioxide Atmospheres," *Ind. Eng. Chem. Process Design Develop.*, **16**, No. 1, 20 (1977).

Dutta, S., and C. Y. Wen, "Reactivity of Coal and Char. 2. In Oxygen-Nitrogen Atmospheres," *ibid.*, 31 (1977).

Hashimoto, K., K. Miura, F. Yoshikawa and I. Imai, "Change in Pore Structure of Carbonaceous Materials During Activation and Adsorption Performance of Activated Carbon," *ibid.*, **18**, 73 (1979).

Hashimoto, K., and P. L. Silveston, "Gasification: Part I. Isothermal, Kinetic Control Model for a Solid With A Pore Size Distribution," *AIChE J.*, **19**, 259 (1973).

Ishida, M., and C. Y. Wen, "Comparison of Zone-Reaction Model and Unreacted-Core-Shrinking Model in Solid-Gas Reactions," *Chem. Eng. Sci.*, **26**, 1031 (1971).

Kawahata, M., and P. L. Walker, "Mode of Porosity Development in Activated Anthracite," in *Proceedings of the Fifth Carbon Conference*, Vol. 2, pp. 251-263, Pergamon Press, New York (1962).

Lacey, D. T., J. H. Bowen and K. S. Basden, "Theory of Non-Catalytic Gas-Solid Reactions," *Ind. Eng. Chem. Fundamentals*, **4**, 275 (1965).

Mendoza, E., R. E. Cunningham and J. J. Ronco, "Oxidation of Zinc Sulfide Pellets—Application of a Model of Diffusion with Simultaneous Reaction under Effective Diffusivity and Surface Area Profiles," *J. Catalysis*, **17**, 277 (1970).

Park, J. Y., and O. Levenspiel, "The Crackling Core Model for the Reaction of Solid Particles," *Chem. Eng. Sci.*, **30**, 1207 (1975).

Petersen, E. E., "Reaction of Porous Solids," *AIChE J.*, **3**, 442 (1957).

Ramachandran, P. A., and J. M. Smith, "A Single-Pore Model for Gas-Solid Non-Catalytic Reactions," *ibid.*, **23**, 353 (1977).

Szekely, J., and J. W. Evans, "A Structural Model for Gas-Solid Reactions with a Moving Boundary," *Chem. Eng. Sci.*, **25**, 1091 (1970).

———, "Studies in Gas-Solid Reactions: Part II. An Experimental Study of Nickel Oxide Reduction with Hydrogen," *Met. Trans.*, **2**, 1699 (1971).

Szekely, J., C. I. Lin and H. Y. Sohn, "A Structural Model for Gas-Solid Reactions with a Moving Boundary—V. An Experimental Study of the Reduction of Porous Nickel-Oxide Pellets with Hydrogen," *Chem. Eng. Sci.*, **28**, (1973).

Szekely, J., J. W. Evans and H. Y. Sohn, *Gas-Solid Reactions*, Academic Press, London, England (1976).

Takamura, T., K. Yoshida and D. Kunii, "Kinetic Study of Oxidation of Zinc Sulfide Pellets," *J. Chem. Eng. Japan*, **7**, 276 (1974).

Tompkins, F. C., "Decomposition Reactions," in *Treatise on Solid State Chemistry: Volume 4. Reactivity of Solids*, N.B. Hannay, ed., Plenum Press, New York (1976).

Walker, P. L., and E. Raats, "Changes in Physical Properties of

Graphitized Carbon Rods upon Gasification with Carbon Dioxide," *J. Phys. Chem.*, **60**, 364 (1956).
Yamada, S., M. Oba, T. Hasegawa, K. Ogawa and Y. Kotera, "The Mechanical Strength of Heterogeneous Catalyst I., The Tensile Strength of Pelletized Alumina Catalysts," *J. Catalysis*, 19, 264 (1970).
Young, D. A., *Decomposition of Solids*, Pergamon Press, Oxford, England (1966).

Manuscript received April 16, 1979; revision received July 20, and accepted August 20, 1979.

Application of Corresponding States Principles for Prediction of Self-Diffusion Coefficients in Liquids

A corresponding states approach has been used successfully to correlate reduced self-diffusivity of pure liquids with reduced temperature and acentric factor. In addition, dimensional analysis techniques have been used to accurately relate viscosity, normal boiling point and temperature with self-diffusivity, as well as to relate the three transport properties.

MOHAMMAD R. RIAZI
and
THOMAS E. DAUBERT
Department of Chemical Engineering
The Pennsylvania State University
University Park, Pennsylvania 16802

SCOPE

In the study of the transport properties of mixtures of liquids, considerable effort has been devoted to the coefficient of mutual diffusion from both the experimental and the theoretical points of view. On the theoretical side, a number of equations have been proposed relating the mutual diffusion coefficient to self-diffusion coefficient and activity of each component in the mixture (McCall and Douglass, 1967; Loflin and McLaughlin, 1968; Skelland, 1974). A number of relationships between self-diffusion coefficients and viscosities of liquids have been proposed in the literature (Li and Chang, 1955; Dullien, 1972).

As diffusivity and thermal conductivity have not been so related, the first purpose of this study is to propose new relationships between diffusivity and easily measurable properties such as boiling point and viscosity with reasonable accuracy. A correlation relating diffusivity to both thermal conductivity and viscosity is also desirable.

The second purpose of this study is the derivation of a corresponding states approach for the prediction of self-diffusion coefficients as has previously been done for viscosity and thermal conductivity.

CONCLUSIONS AND SIGNIFICANCE

Beginning with dimensional analysis a relationship between self-diffusivity, viscosity, boiling point and temperature has been derived which predicts self-diffusivity with an average error of 2 to 3%:

$$\frac{\mu^{2/3}}{T} D = 6.35 \times 10^{-8} (T/T_b)^{0.83}$$

By a similar approach, a relationship between the three transport properties (viscosity, thermal conductivity and diffusivity) has been derived with a mean deviation of ±3.5%:

$$\sqrt{\frac{K}{v_s^3}} D = 4.65 \times 10^{-4} \left(\frac{KT}{v_s^2 \mu}\right)^{0.979}$$

It has been shown that the corresponding states principle is applicable to prediction of diffusivity. Using the generalized correlation for diffusivity developed in this work, an average error of 4.5% was obtained for twenty systems in the prediction of self-diffusion coefficients of pure liquids. The generalized correlations also can be used to predict diffusivity of a liquid at any temperature if diffusivity is known at one temperature:

$$D_r = (0.4 - \omega) D_r^{(1)} + (\omega - 0.2) D_r^{(2)}$$

where $D_r^{(1)}$ and $D_r^{(2)}$ are functions of reduced temperature.

Correspondence concerning this paper should be addressed to Thomas E. Daubert.

0001-1541-80-3683-0386-$00.75.